

Single Nanoparticle Electrocatalysis: Effect of Monolayers on Particle and Electrode on Electron Transfer

Xiaoyin Xiao,[†] Shanlin Pan,[‡] Jum Suk Jang, Fu-Ren F. Fan, and Allen J. Bard*

Center for Electrochemistry, Department of Chemistry and Biochemistry, University of Texas at Austin, 1 University Station A5300, Austin, Texas 78712-0165

Received: May 22, 2009; Revised Manuscript Received: July 7, 2009

The electrocatalytic properties of individual single Pt nanoparticles (NPs) can be studied electrochemically by measuring the current–time ($i-t$) responses during single NP collisions with a noncatalytic ultramicroelectrode (UME). The Pt NPs are capped with citrate ions or a self-assembled monolayer (SAM) of alkane thiols terminated with carboxylic acid that affect the observed $i-t$ responses. By varying the length of the SAMs or the composition of a mixed monolayer, we have studied the effect of adsorbed molecules on the catalytic activity of Pt NPs at the single particle level through electrocatalytic amplification of single NP collisions. Collisions of single NPs were triggered and recorded as individual current steps whose amplitude represents the reactivity of single Pt NPs for the reaction of interest, here hydrazine oxidation, at a given electrode potential. The catalytic properties of Pt NPs are dependent not only on the nature of the interaction between the adsorbed monolayer and the catalytic NP surface, but also on the rate of electron transfer through the SAMs, governed by their length.

Introduction

We have previously described a technique for studying electrocatalytic reactions on single nanoparticles (NPs) by observing the current that flows when the NP collides with and sticks to an electrode that itself does not carry out the reaction of interest (e.g., proton reduction or hydrazine oxidation).^{1,2} The inert ultramicroelectrode (UME), e.g. a C fiber, is held at a potential where the reaction does not occur. However when a Pt NP collides with it, the reaction can take place at a rate determined by the concentration of reactant in solution, its diffusion coefficient, the potential, and the available reaction area on the NP. Nanoparticles are widely used as heterogeneous catalysts by providing a high number of surface atoms to volume ratio and, thus, a high density of active sites.^{3–7} Both particle size and shape have been found to play important roles in their reactivity and selectivity. A variety of methodologies has been developed to control particle size, shape, and crystallinity. For example, multiple faceted, highly active Pt nanocrystals can be prepared by electrochemical deposition on a glassy carbon electrode followed by square wave potential treatment.⁸ The modulation of the electrode potential led to particle growth selectively at specific surface locations. The nanocrystals prepared did not require surfactant molecules or capping agents for stabilization of size and shape. In general, however, NPs are made by colloidal synthetic methods that require the use of stabilizing molecules to have better control over the particle nucleation and growth process, and to prevent aggregation and particle growth on storage. The stabilizing molecules are often long alkyl chain species with thiol, amine, or carboxylic acid end groups, dendrimers, or polymers. These capping agents can affect the catalytic properties of the surface and also, of interest

in collision studies, how well the particles stick to a surface. Removal of these stabilizers represents a significant challenge since these organic molecules are usually strongly bound to the NP surfaces at approximately full monolayer coverage. In this work, we will describe a simple, fast, and reliable method to study these effects: through electron transfer through the SAMs and the occupation of the active sites for inner sphere reactions by surface adsorption.

Experimental Section

Most of the experimental procedures follow those reported in our earlier studies.^{1,2} The Pt NPs were prepared by reducing H_2PtCl_6 precursor in the presence of sodium citrate using sodium borohydride, as in earlier studies. The size of Pt NPs ranged from 3 to 5 nm, with the size distribution centered at ~ 3.6 nm in diameter. The as-prepared Pt NPs were capped with citrate ions. The particles were then capped by alkane thiols terminated with carboxylic acid through ligand replacement, which was accomplished by mixing the as-prepared Pt NPs with C3 (3-mercaptopropanoic acid), C6 (6-mercaptophexanoic acid), C8 (8-mercaptooctanoic acid), C12 (12-mercaptododecanoic acid), or C16 (16-mercaptohexadecanoic acid) at different particle to alkane thiol molar ratios, respectively (all chemicals are from Sigma Aldrich). After the overnight replacement reaction, the solution was filtered through a $0.2 \mu\text{m}$ filter to remove aggregates above 200 nm. In the electrochemical studies, a gold UME ($10 \mu\text{m}$ diameter) was used as the working electrode. It was mechanically polished and electrochemically cleaned by cycling the electrode between the potentials where the surface oxidation and reduction occurs in 0.1 M HClO_4 . The electrochemical equipment was the same as reported in previous studies.^{1,2}

The surface assembly of C3, C6, C8, C12, and C16 on the Au UMES was performed electrochemically by cycling the electrode potential 5 times between -0.4 and $+0.6 \text{ V}$ vs SHE in their test electrolytes containing hydrazine. By simply

* Corresponding author. E-mail: ajbard@mail.utexas.edu.

[†] Present address: Air Force Research Laboratory, Materials and Manufacturing Directorate, Wright-Patterson Air Force Base, Dayton, OH 45433-7707.

[‡] Present address: The University of Alabama, Department of Chemistry, Tuscaloosa, AL 35487-0336.

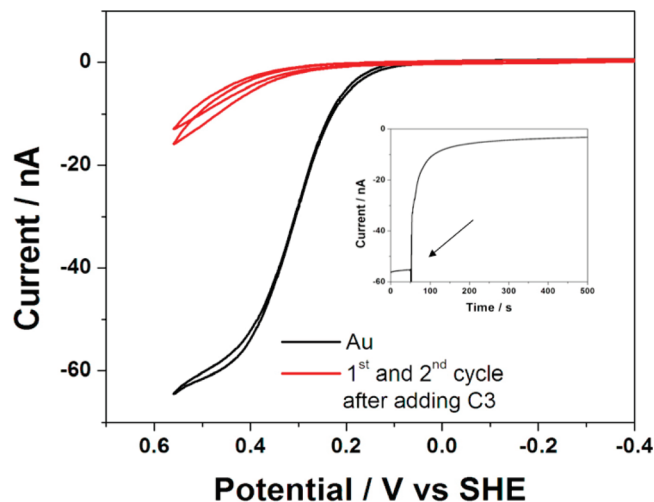


Figure 1. Cyclic voltammograms at Au UME in 12 mM hydrazine + 50 mM PBS before and after adding 50 μM 3-mercaptopropionic acid (C3): scan rate 100 mV/s. The inset figure shows the current transient before and after injection at 0.45 V.

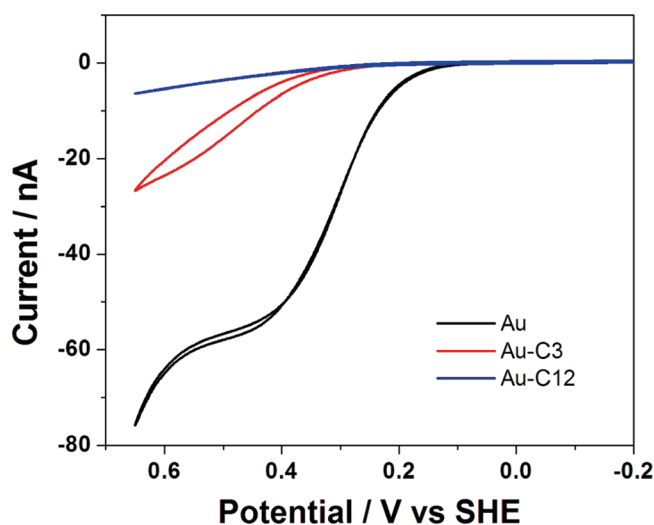


Figure 2. Cyclic voltammograms at Au UME in 12 mM hydrazine + 50 mM PBS before and after adding 10 μM 3-mercaptopropionic acid (C3) and 12-mercaptododecanoic acid (C12), respectively: scan rate 100 mV/s.

immersing Au UMEs in ethanol containing those molecules overnight, we found that the extent of coverage was much less than those obtained from the electrochemically assisted assembling processes.^{9–11}

Results and Discussion

Heterogeneous Inner Sphere vs Outer Sphere: Effect of SAMs. When alkane thiol molecules are assembled at the electrode surface, the surface coverage can be simultaneously determined from the suppression of hydrazine oxidation. As shown in Figure 1, hydrazine oxidation was suppressed dramatically even in the first potential cycle as compared with the oxidation before adding C3 molecules. The current was further slightly decreased in sequential cycles, suggesting that the initial adsorption was much faster than that of surface self-assembly processes. Figure 2 shows the sixth potential cycle after adding C3 or C12. Hydrazine oxidation was significantly suppressed, even by C3, with the onset for oxidation shifted positively by about 100 mV in both cases. The oxidation current was much smaller when the Au surface was covered by C12. Note that

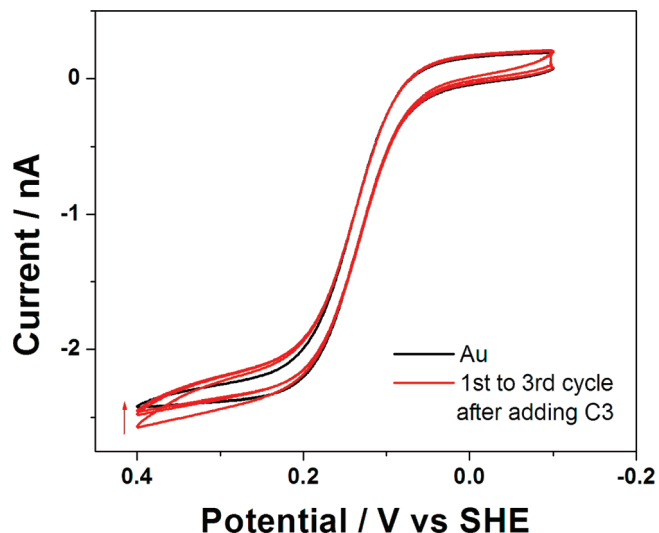


Figure 3. Cyclic voltammograms at Au UME in 1 mM ferrocenemethanol + 50 NaClO₄ before and after adding 50 μM 3-mercaptopropionic acid (C3): scan rate 100 mV/s.

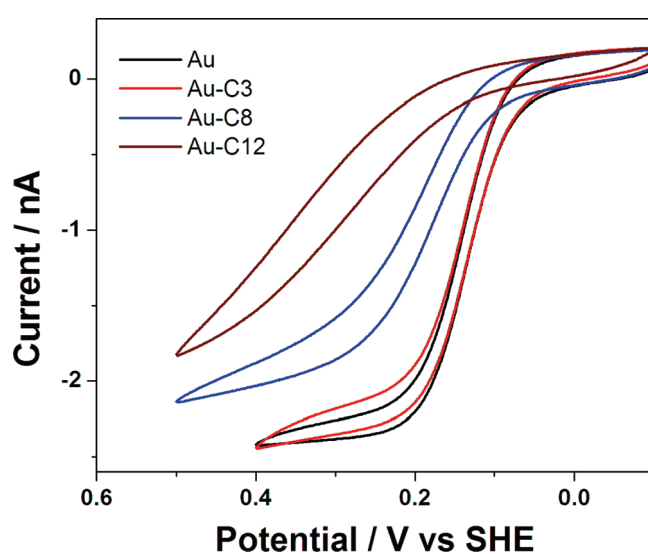


Figure 4. Cyclic voltammograms at Au UME in 1 mM ferrocenemethanol + 50 mM NaClO₄ before and after adding 10 μM 3-mercaptopropionic acid (C3), 8-mercaptooctanoic acid (C8), and 12-mercaptododecanoic acid (C12), respectively: scan rate 100 mV/s.

the scan in both forward and backward directions is almost overlapping as a straight line, an indication of more complete coverage of C12 as compared to the C3 monolayer. Since even C3 should totally suppress the electrocatalytic hydrazine oxidation process, this suggests that the C3 film still has defects that allow the reaction to proceed, as opposed to the C12 film.

While the heterogeneous inner sphere oxidation of hydrazine that involves strong involvement of the electrode surface material is blocked by C3, the heterogeneous outer sphere redox process of ferrocenemethanol (FcMeOH) is essentially unaffected, as shown in Figure 3. However, as is well-known, the longer carbon chain alkane thiols, C6, C8, and C12, respectively, do suppress the oxidation of FcMeOH as revealed by the decrease in the oxidation current and the positive shift of half-wave potentials (Figure 4). The longer the carbon chain length, the larger the shift in the oxidation potential. This effect is mainly due to the suppression of electron tunneling through SAMs.^{10–13}

These results demonstrate that SAMs play significantly different roles for heterogeneous inner sphere and outer sphere

reactions. When the catalytic particles are stabilized by SAMs, the stabilizing molecules may occupy the surface active sites, leading to not only blockage of surface reactions but also suppression of the reaction rates through length-dependent electron transport within the SAMs. Since there is no electrocatalytic amplification for outer sphere reactions, the heterogeneous inner sphere reaction, hydrazine oxidation, is the main focus in our single particle collision experiments. To differentiate the above assumed two roles of SAMs on particle activity, the experiments were carried out in the following two strategies: (1) collisions of Pt NPs at Au UMEs covered by SAMs and (2) collisions of Pt NPs covered by SAMs at clean Au UMEs.

In the following two sections, we determine the catalytic activity of Pt NPs by monitoring the hydrazine oxidation current generated in the event of single NP collisions. The details of the principles and the experimental procedures can be found elsewhere.^{1,2} A brief description is given here. Hydrazine oxidation does not occur at Au electrodes at a potential around 0.1 V but occurs at significantly higher rates at Pt electrodes at this potential. Therefore, when individual Pt NPs adsorb on a Au electrode, hydrazine oxidation is turned on, resulting in individually corresponding current transients. The frequency of particle collisions is controlled by injecting a very low concentration of particle solution into the test electrolytes. When the concentration is sufficiently low, a few picomolar, collision of single particles one at a time could be observed as random current transients. The amplitude of each current is a function of the particle size and the kinetics of electrocatalytic reaction at the particle surfaces. In general, the currents at several electrode potentials can be used to determine the kinetics for single Pt NPs, but here, we only compare the current at the same electrode potential among the Pt NPs modified in different ways.

Collisions of Pt Particles at Au Electrodes Modified with SAMs. The as-prepared Pt NPs stabilized by citrate ions were used to determine the suppression of electron tunneling through SAMs to the NPs. In this case, the Pt NP surfaces remained active, but the electron tunneling distance from the electrode to the NP was varied by SAMs of different lengths (Figure 5a). The Au UMEs were electrochemically modified with C3, C6, C8, C12, or C16 monolayers, as described above. The potential of these modified electrodes was then held at 0.1 V, where essentially no hydrazine oxidation occurs on Au as shown in Figures 1 and 2. As shown in Figure 5c, the oxidation current gradually increased after injecting the Pt colloid solutions. The electronic noise at about 20 s was due to the opening and closing of the Faraday cage for particle injection. The increase in oxidation current was due to the collision and adsorption of Pt NPs, which were more catalytic than the Au electrodes for hydrazine oxidation. Note that the current increased in a stepwise fashion, signaling individual adsorption events. In each current–time ($i-t$) curve, the current in each individual transient was somewhat different, indicative of variable activity of Pt NPs adsorbed at the Au electrode modified with the SAM. At clean Au electrodes, the current was strongly correlated to the size of Pt NPs when they were capped by only citrate ions. The current step was mostly between 40 and 55 pA with a few larger ones. We have assigned these large current steps to the collisions of particle aggregates.² While theory predicts, and we have sometimes seen current transients that remain fairly constant, we also see transients where the current decays slowly (over several seconds) after the initial rise.^{1,2} This has been ascribed to deactivation of the particles, e.g. by adsorption of adventitious impurities.

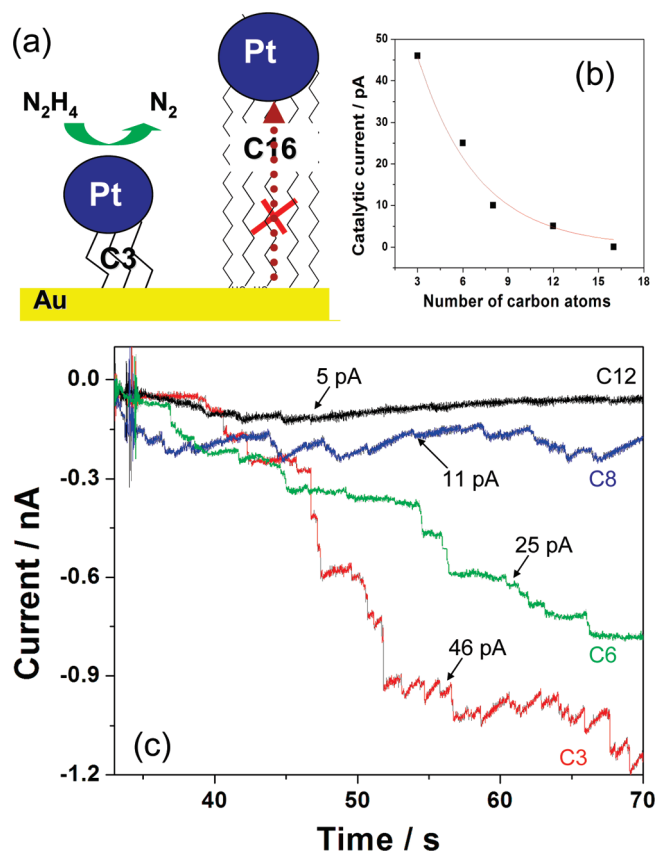


Figure 5. Collisions of Pt NPs at SAM-covered Au electrodes. (a) Schematic illustration of particle collisions at the SAMs: catalytic hydrazine oxidation and suppression of electron transport through long molecular spacers. (b) Plot of representative catalytic current versus the number of carbon atoms in SAMs. (c) Current transients recorded at different SAMs. Au electrode 10 μ m in diameter, electrode potential 0.1 V, particle size \sim 3.6 nm, particle concentration 50 pM, electrolyte 12 mM hydrazine + 50 mM PBS buffer, pH \sim 7.5.

When the Au electrodes were covered by SAMs, the collision of Pt NPs can take place on top of the well-assembled monolayer or at defects within the monolayer of a size that the NP can penetrate. During SAM preparation the oxidation current for hydrazine did not decrease further after about five potential cycles, meaning that the SAM probably attained near limiting monolayer surface coverage. The typical $i-t$ curves recorded on these modified Au UMEs are shown in Figure 5c. The current in individual current transients was dramatically decreased when the SAM chain length was increased, leading also to slower increase of the current over the experimental recording time. A very small percentage of large current steps shown in each $i-t$ curve might be due to either single collisions of individual large particle aggregates or multiple single particle collisions, which are not well resolved temporally. The current did not show any significant change when the Au electrode was covered by the C16 monolayer before and after injecting Pt NPs (not shown). Even with C12, the currents were still within the signal-to-noise level. With the other shorter chain SAMs, the current steps were distinguishable from both $i-t$ curves and their corresponding first-order derivatives. The currents indicated for each curve in Figure 5c represent the amplitude of the majority of the current steps. We thus used these numbers to plot the catalytic current versus carbon chain length of SAMs (i.e., number of carbons in the monolayer). The plot shows an exponential decay (see Figure 5b). The decay resembles the exponential decay of electron transport through SAMs. The distance factor for

extended charge transfer, β , can be estimated to be ~ 0.5 $1/\text{\AA}$ by assuming that each C–C single bond has an effective bond length of 0.5 \AA ; this is about half of the β value found for through-bond electron tunneling for electroactive groups bound on saturated alkyl chains, which has a typical β value in the range of 1 – 1.2 $1/\text{\AA}$.¹⁴ The smaller β value may be due to relatively large particle size as compared to the assembled single molecules, i.e., one Pt NP may contact with multiple molecules in the formed NP-molecule–Au substrate junction. It may also be caused by less well-ordered SAMs, especially with the shorter alkylthiols with a closer approach than that suggested by the alkyl chain length. This work suggests that electrons can tunnel through the monolayer to the Pt NP for hydrazine oxidation to occur at the surface of Pt NPs. Very few techniques have been developed to determine the electron transport properties of organic molecules at the single molecule or surface assembled monolayer level.^{15–17} This technique thus provides a simple way to determine the rate of electron transport through SAMs using individual single catalytic NPs.

Collisions of Pt Particles Modified with SAMs at Clean Au Electrodes. When Pt NPs were stabilized by citrate ions, the citrate ions are strongly solvated with water molecules, so the electrocatalytic activity of Pt NPs for hydrazine oxidation is largely maintained. When mixed with the studied thiolated molecules, the weak electrostatic interaction between Pt and citrate ions is replaced by stronger covalent Pt–S bonds, with the terminal carboxylic groups pointing toward the electrolyte. These thiolated SAMs are strongly adsorbed at the Pt surfaces and, therefore, prevent hydrazine from adsorbing and dissociating at the catalytic surface, leading to strong suppression of electrocatalytic activity of Pt NPs toward the heterogeneous inner sphere reaction. The strong suppression of hydrazine oxidation has already been shown in Figures 1 and 2 at Au electrodes. Similar characteristics have also been recorded at Pt UMEs.

C3 can partially replace citrate ions when mixing Pt NPs with C3 at small C3-to-particle ratios. Increasing the ratio results in a larger surface coverage of C3 relative to citrate. Figure 6 shows the electrocatalytic activity of Pt NPs covered by a mixed monolayer of C3 and citrate ions. The Pt NPs lost their activity as more C3 was adsorbed on the NP surface. The current increase is negligible at a ratio above 2000, indicating that the heterogeneous hydrazine oxidation is totally inhibited when C3 completely occupies the catalytic surface of Pt NPs. The activity of such Pt NPs could be recovered by cycling the electrode to very positive potentials, e.g., 1.2 V, because of anodic stripping of C3 at the positive electrode potentials. The decrease in particle activity is thus attributed to the occupation of catalytic active sites on the Pt NP surface. On the other hand, as discussed in the first section, the C3 short chain does not appreciably hinder the electron transfer in a heterogeneous outer sphere reaction.

The replacement of citrate ions by longer SAMs led to a larger and quicker decrease in particle activity. Figure 7 shows the current transients recorded before and after injecting Pt NPs covered by a mixed monolayer of C12 and citrate ions. Mixing of Pt NPs with C12 at a 1:100 molar ratio led to complete suppression of hydrazine oxidation. The longer the carbon chain of the SAM, the lower the concentration of SAM that is needed to completely prevent hydrazine oxidation at the Pt NP surfaces, because longer chain alkyl thiols are more strongly adsorbed and form more compact monolayers, in addition to inducing larger suppression of the electron tunneling process.

We have also studied other stabilizing molecules, such as polyvinylpyridine (PVP), cetyltrimethylammonium bromide

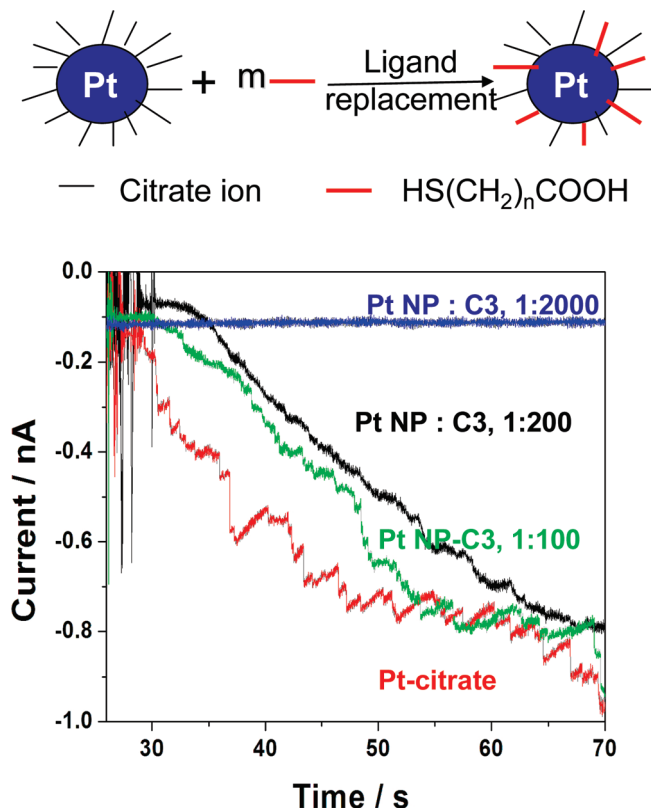


Figure 6. Current transients recorded at Au UMEs before and after injection of Pt nanoparticles capped by a mixture of citrate ions and C3 SAMs. Replacement of citrate by SAMs is illustrated at the top of the figure. Au UMEs 10 μm in diameter, electrode potential 0.1 V, particle size ~ 3.6 nm, particle concentration ~ 50 pM, electrolyte 12 mM hydrazine + 50 mM PBS buffer, pH ~ 7.5 .

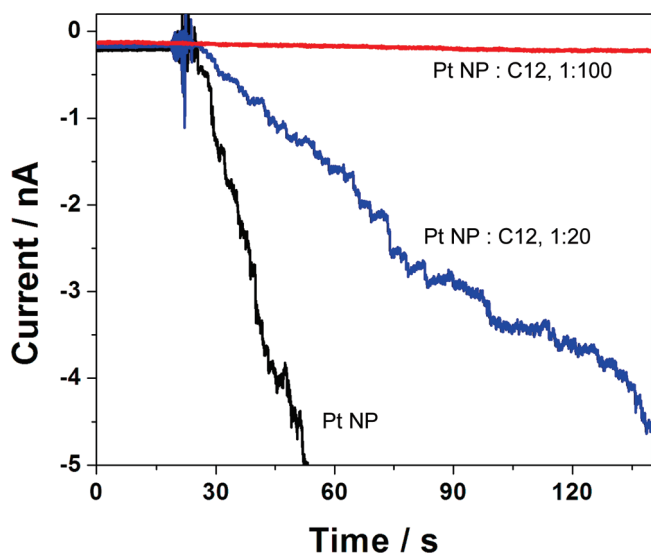


Figure 7. Current transients recorded at carbon UMEs before and after injection of Pt NPs capped by a mixture of citrate ions and C12 SAM. C UME 8 μm in diameter, electrode potential 0.45 V, Pt NPs ~ 3.6 nm, particle concentration 50 pM, electrolyte 12 mM hydrazine + 50 mM PBS buffer, pH ~ 7.5 .

(CTAB), and DNA single strands. The as-prepared Pt NPs lose the hydrazine reactivity when mixed with a few millimolar (i.e., 5 mM) of PVP or CTAB. Further rinsing the PVP or CTAB capped Pt NPs with 10 mM sodium citrate solution would partially recover particle reactivity. Note that the presence of PVP and CTAB in the electrolyte does not effectively affect

the hydrazine reactivity at Pt or Au UMEs. Adsorption of thiolated single strand and double strand DNA showed similar loss of activity. We are currently pursuing detailed studies of the dependence of particle activity on the DNA hybridization processes.

In conclusion, we have demonstrated here in single NP collision experiments that organic molecules adsorbed on the NP surface can affect the electrocatalytic oxidation of hydrazine. The kinetics of hydrazine oxidation at Pt NPs is dependent on the SAM adsorbed on either a Au working UME or Pt NPs. In the first strategy, the Pt NPs are only capped with citrate ions, while the working electrode is covered by SAMs of different carbon chain length. We found that the electron transfer rate of redox molecules was decreased exponentially with the increase of the alkyl chain length of the SAM for both inner and outer sphere reactions. The decrease of the overall particle activity is mainly limited by the exponential decay of electron transport from Pt NPs through SAMs to the Au surface. In the second strategy, the Pt NPs are capped by SAMs or the mixture of SAMs and citrate ions, while the working electrode remains clean. We found that the electrocatalytic activity of Pt NPs for hydrazine oxidation gradually decreased with an increase in the concentration of the SAM (of the same carbon chain length). The decrease of particle activity is mainly due to the blockage of the catalytic surface sites toward inner sphere reactions. This work continues the development of a quick and reliable method to screen the catalytic activity of NPs at the single particle level using electrocatalytic amplification.

Acknowledgment. We acknowledge support from the National Science Foundation (CHE 0451494 and CHE 0808927)

and the Robert A. Welch Foundation (F-0021). We appreciate valuable discussions with Drs. Steve Feldberg and Cynthia Zoski.

References and Notes

- (1) Xiao, X. Y.; Bard, A. J. *J. Am. Chem. Soc.* **2007**, *129*, 9610–912.
- (2) Xiao, X. Y.; Fan, F.-R. F.; Zhou, J.; Bard, A. J. *J. Am. Chem. Soc.* **2008**, *130*, 16669–16677.
- (3) (a) Narayanan, R.; El-Sayed, M. A. *Chimica OGGI-Chem. Today* **2007**, *25*, 84–86. (b) Narayanan, R.; El-Sayed, M. A. *J. Phys. Chem.* **2005**, *109*, 12663–12676.
- (4) Bratlie, K. M.; Lee, H.; Komvopoulos, K.; Yang, P. D.; Somorjai, G. A. *Nano Lett.* **2007**, *7*, 3097–3101.
- (5) Polsky, R.; Gill, R.; Kaganovsky, L.; Willner, I. *Anal. Chem.* **2006**, *78*, 2268–2271.
- (6) Yang, J.; Lee, J. Y.; Too, H. P. *Anal. Chim. Acta* **2006**, *571*, 206–210.
- (7) Rao, V.; Simonov, P. A.; Savinova, E. R.; Plaksin, G. V.; Cherepanova, S. V.; Kryukova, G. N.; Stimming, U. *J. Power Sources* **2005**, *145*, 178–187.
- (8) Tian, N.; Zhou, Z. Y.; Sun, S. G.; Ding, Y.; Wang, Z. L. *Science* **2007**, *316*, 732–735.
- (9) Diao, P.; Guo, M.; Hou, D.; Xiang, M.; Zhang, Q. *J. Phys. Chem. B* **2006**, *110*, 20386–20391.
- (10) Sabatini, E.; Gafni, Y.; Rubinstein, I. *Langmuir* **1993**, *9*, 3660–3667.
- (11) Cai, L.; Yao, Y.; Yang, J.; Price, D. W.; Tour, J. M. *Chem. Mater.* **2002**, *14*, 2905–2909.
- (12) Xiao, X. Y.; Nagahara, L. A.; Rawlett, A. M.; Tao, N. J. *J. Am. Chem. Soc.* **2005**, *127*, 9235–9240.
- (13) Feldberg, S. W.; Newton, M. D.; Smalley, J. F. *Electroanalytical Chemistry*; Bard, A. J., Rubinstein, I., Eds.; Marcel Dekker: New York, 2004; Vol. 22, pp 102–180.
- (14) Finklea, H. O. *Electroanal. Chem.* **1996**, *19*, 120, and references cited therein.
- (15) Ulgut, B.; Abruna, H. D. *Chem. Rev.* **2008**, *108*, 2721–2736.
- (16) Bumm, L. A. *ACS Nano* **2008**, *2*, 403–407.
- (17) Tao, N. J. *Nat. Nanotech.* **2006**, *1*, 173–181.

JP904811F